IEEE Open Journal of
Vehicular Technology

Received 22 April 2020; accepted 10 May 2020. Date of publication 14 May 2020;
date of current version 3 June 2020. The review of this article was arranged by Associate Editor K.-C. Chen.

Digital Object Identifier 10.1109/OJVT.2020.2994626

Design of Digital Communications for Strong Phase Noise Channels

SIMON BICAÏS AND JEAN-BAPTISTE DORÉ

CEA-Leti , Grenoble 38054, France

CORRESPONDING AUTHOR: SIMON BICAÏS (e-mail: simon.bicais@cea.fr)

This work was supported by the French National Research Agency (ANR-17-CE25-0013) within the frame of the project BRAVE.

ABSTRACT To meet the requirements of beyond 5G networks, the significant amount of unused spectrum in sub-TeraHertz frequencies is contemplated for high-rate wireless communications. Yet, the performance of sub-TeraHertz systems is severely degraded by strong oscillator phase noise. We investigate in this paper the design of digital communications robust to phase noise. This problem is addressed in three steps: the characterization of the phase noise channel, the design of the optimum receiver, and the optimization of the modulation scheme. This paper proposes a joint performance and implementation optimization. First, we address the design of the demodulation scheme for phase noise channels and propose the polar metric, a soft-decision rule for symbol detection. It is shown that performance gains are achieved for coded and uncoded systems with valuable complexity reductions of the receiver. Second, we investigate the optimization of the modulation scheme for phase noise. We demonstrate that using a constellation defined upon a lattice in the amplitude-phase domain leads to significant performance gains and a low-complexity implementation. Thereupon, we propose the Polar-QAM scheme with efficient binary labeling and demodulation. Numerical simulation results show that the proposed modulation and demodulation schemes offer valuable solutions to achieve high-rate communications on systems strongly impaired by phase noise.

INDEX TERMS Sub-TeraHertz communications, phase noise, maximum likelihood detection, channel estimation, constellation, binary labeling.

I. INTRODUCTION

With a specific demand for wireless connectivity, the current exponential data traffic growth will require within few years data rates above 100+ Gbit/s. To reach this requirement additional breakthrough technologies are necessary, and hence, several key approaches are under investigation, such as massive multiple-inputs multiple-outputs systems, cell densification, etc. In particular, the aggregation of more spectrum is considered as one of the foremost solutions to meet the requirements of future wireless applications. For these reasons, the interest in wireless communications in frequencies above 90 GHz is continuously growing [1]. *Sub-TeraHertz* (sub-THz) frequencies from 90 to 300 GHz offer a significant amount of unused spectrum [2] and therefore represent a true opportunity to achieve high data-rate wireless communications. Sub-THz communications are contemplated in order to meet the requirement of both terrestrial and vehicular beyond 5G networks as described in [3] and [4]. Some of the contemplated scenarios for sub-THz communications [2] are high capacity back-hauling, device-to-device communications and Gbit/s vehicular-to-vehicular communication systems [4]. Nonetheless, additional researches are required to design efficient and new physical layer algorithms. Traditional techniques cannot be directly transposed to sub-THz bands as they do not consider the unique features of radio-frequency (RF) impairments of sub-THz systems. In particular, they suffer from strong phase impairments due to the poor performance of high-frequency oscillators [2], [3]. State-of-the-art approaches [2] investigate the use of coherent systems together with channel bonding. This type of architecture needs to be further combined with signal processing optimization to mitigate the effects of phase impairments. Therefore, one challenge to be addressed for sub-THz systems is the design of robust communications impaired by strong phase noise (PN).

Assuming a PN channel, the performance of sub-THz communication systems can be improved from both receiver

and transmitter sides. First, the receiver algorithms may be adapted to PN channels. An appropriate decision rule for symbol detection is to improve the demodulation performance. It has motivated extensive work on the design of optimum decision rules for systems impacted by PN. The optimum receivers for common PN models are listed in [5]. However, detectors of the literature present complex definitions making the practical implementation challenging, particular when soft-decision decoding is considered. Current communication systems are combined with soft-decision decoding known to improve significantly the demodulation performance. Still, the computability of probabilistic bit values, namely log-likelihood ratios (LLR), has rarely been studied in the literature and should be a prime consideration in this problem. Second, the performance of communication systems may also be enhanced through the optimization of the signal constellation for PN. Choosing M points in a two-dimensional space such that a target function is optimized is a widely investigated problem. In particular, there exists an extensive amount of literature on constellation optimization for PN channels. The following articles are representative of prior work. Research on constellation optimization for PN has begun fifty years ago with Foschini in [6] where signal points are selected among a lattice with a heuristic search to minimize the symbol error probability (SEP) for Tikhonov PN. More recent works have exploited powerful numerical optimization algorithms such as simulated annealing [7] or gradient-search [5] to maximize the mutual information (MI) or minimize the SEP. The work in [8] optimizes amplitude-phase-shift keying (APSK) constellations with a simplex algorithm to minimize the SEP for non-linear PN. The state-of-the-art solution on constellation optimization for Gaussian PN is proposed in [9]: The spiral constellation based on a semi-analytical description, i.e. the modulation points are defined with a closed-form expression upon an optimized modulation shape parameter. Nevertheless, most of the constellations proposed in the literature are efficient but local solutions. These schemes are optimized for a specific signal-to-noise ratio (SNR) and PN variance, and thus, does not describe a comprehensive solution. Furthermore, existing solutions are often unstructured which leads to difficult practical implementation with complex binary labeling and demodulation. In contrast to prior work, we investigate in this paper a joint optimization of communication performance and implementation on practical systems.

The contributions of this paper are the following. First, we detail the system model for sub-THz communication systems. Based on the results of recent measurement campaigns, the sub-THz propagation channel is described with a line-of-sight (LoS) model. Moreover, we model accordingly to [10] the impact of PN with a Gaussian process. Second, we investigate the design of the optimum demodulation scheme for the Gaussian phase noise (GPN) channel. We also introduce the *polar metric*, a low-complexity detection scheme minimizing the error probability. The proposed detector achieves, with a simpler implementation, the optimum detection performance of the state-of-the-art detector described in [5]. We also propose a low-complexity implementation of the soft-output demapper using the polar metric for soft-decision channel decoding. Our results demonstrate that using the proposed polar metric leads to important performance gains and significant complexity reductions of the receiver implementation. Third, the optimization of the modulation scheme for the GPN channel is addressed. This paper provides an original mathematical framework to design PN robust constellations based on a signal decomposition in polar coordinates. An analytical approach is conducted to demonstrate how optimal constellations can be built to maximize performance on the GPN channel. Motivated by this theoretical analysis, we propose the *polar quadrature amplitude modulation* (PQAM or Polar-QAM), a PN robust modulation scheme based on a structured APSK. The constellation and the binary labeling of the Polar-QAM are jointly designed to improve the system performance on PN channels while maintaining a low-complexity implementation. In particular, it enables to implement the symbol detection with a simple threshold comparison, and the soft-output demapper with piecewise linear functions. The proposed modulation scheme is compared to conventional and state-of-the-art solutions taking into account different performance metrics. The performance of the Polar-QAM is assessed analytically and numerically considering state-of-the-art channel codes. Our results highlight that the Polar-QAM significantly enhances performance in terms of achievable data rate with valuable complexity reductions of the transceiver. Moreover, we present a new link adaptation technique particularly adapted to the wide spectrum covered by envisaged sub-THz applications. Thanks to the regular structure of the Polar-QAM, the proposed modulation scheme can be easily adapted to the SNR and PN variance, and hence, provides a general solution to various channel conditions.

The main contribution of this paper is to propose a comprehensive optimization of the communication schemes for strong PN channels. Under a transceiver perspective, we investigate and cross-correlate the design of multiple communication schemes including the constellation, the binary labeling, the symbol detection, the soft-output demapper, and the link adaptation strategy. To the best of our knowledge, such extensive optimization has not been addressed in the literature. Moreover, many works on modulation design for PN channels are either based on (i) complex numerical optimizations [5]; or on (ii) semi-analytical approaches [9], namely optimizing a reduced set of parameters to define the modulation. In contrast, our work is supported by an original theoretical framework, based on the signal decomposition in the amplitude-phase domain, providing analytical tools to design PN robust communications and evaluate many of the literature proposals. Altogether, the proposed schemes offer a valuable solution to realize high rate communications on practical systems impaired by strong PN, and thus, to meet the requirements of future sub-THz wireless communication systems.

The remainder of the paper is organized as follows. Section II introduces the system model by detailing the channel

and PN models. In Section III, the design of receiver algorithms for the GPN channel is investigated. Then Section IV is dedicated to the optimization of the modulation scheme and introduces the proposed PQAM scheme. Finally, potential applications and perspectives are outlined in Section V while Section VI concludes the paper.

II. SYSTEM MODEL

A. CHANNEL MODEL

Theoretical expectations that the LoS path provides most of the energy contribution in sub-THz propagation channels have been demonstrated by the recent measurement campaigns within sub-THz bands. The indoor radio propagation channel has been characterized through measurements between 126 and 156 GHz in [11]. Complementary results on non-LoS components can be found in [12]. Sub-THz channels have also been characterized in [13] using deterministic ray-tracing tools. We assume subsequently in this paper a LoS propagation channel model.

A single-carrier coherent communication system[1] impaired by PN is considered. We assume that the effects of the propagation channel are perfectly[2] compensated and that the receiver is synchronized in time and frequency. We therefore study the discrete-time symbol model of a complex additive white Gaussian noise (AWGN) channel impaired by oscillator PN. The received symbol is then given by

$$r = s \cdot e^{j\phi} + n, \tag{1}$$

where s denotes the transmitted symbol and n is a zero-mean circularly symmetric complex Gaussian variable modeling thermal noise, i.e. $n \sim \mathbb{C}\mathcal{N}(0, \sigma_n^2)$. The oscillator PN to be modeled is described by ϕ. Transmitted symbols are modulated with duration T and belong to constellation $\mathcal{C}$ with modulation order M and average energy E_s. The power spectral density of thermal noise n is denoted $N_0/2$ such that $\sigma_n^2 = N_0/2T$. The considered discrete-time symbol model in Eq. (1) has been further characterized in [14]. Conditions on the sampling rate and on the PN intensity of the system are given to ensure the accuracy of this model. In the following, we adopt the polar representation and use subscripts ρ and θ to respectively denote the amplitude and phase of a symbol.

With regard to the propagation channel, it is worth pointing out the following remarks. The model in Eq. (1) can be easily adapted to include the propagation gain and phase shift of a frequency-flat channel with a single dominant path, the envisaged model for sub-THz scenarios. This is achieved by integrating a complex coefficient h as follows $r = h \cdot s \cdot e^{j\phi} + n$, where h varies slowly. If the receiver estimates and compensates the channel coefficient h with sufficient accuracy, then the channel can be described with Eq. (1) in a more concise way. The unique resulting difference in the system model would be the definition of the spectral density of thermal noise which should be modified from $N_0/2$ to $N_0/2|h|^2$. Besides, single or multi-carrier systems communicating on multipath channels and impaired by PN have to be described differently and with more complex models, see [15]. Optimizing communication schemes for multipath channels in the presence of PN exceeds the scope of this paper – readers may refer to [16]. This work targets sub-THz applications and hence focuses on propagation channels with a single dominant path.

B. PHASE NOISE MODEL

In communication systems, the generation of PN in oscillators results from the integration and amplification by the phase-locked loop (PLL) of noise sources within the circuitry [17]. As a result, oscillator PN presents a cumulative and correlated nature. Under the assumption that the oscillator is only subject to white noise, the oscillator PN ϕ can be modeled by the superposition of a correlated Wiener (Gaussian random-walk) process and an uncorrelated Gaussian one [17] respectively expressing the integration and amplification of thermal noise in the PLL. The spectrum of oscillator PN is then described by a colored K_2/f^2 characteristic (Wiener PN) and a white noise floor K_0 (Gaussian PN). Nonetheless, it has been shown in [18] that for high-rate systems the influence of Wiener PN on the communication performance is negligible in comparison to the Gaussian one. In other words, for wide-bandwidth systems, the noise floor of the oscillator is the main contribution to the observed PN. These results have been confirmed in [10] and further characterized through the comparison of a correlated PN model to an uncorrelated one. The main result of this study is that the PN is appropriately modeled by an uncorrelated process if

$$N \cdot f_0^2 \cdot T^2 \leq \frac{\ln(2)}{2\pi^2}, \tag{2}$$

where N is the frame length, f_0 is the corner frequency of the oscillator and T is the symbol duration. Namely, N denotes the number of symbols between two channel estimations and phase corrections. With regard to state-of-the-art sub-THz oscillators and contemplated sub-THz systems parameters [2], it follows that Eq. (2) is easily satisfied. For instance, this condition is satisfied when considering the state-of-the-art oscillator in [19] with $f_0 = 1$ MHz, a system bandwidth $1/T = 1$ GHz and $N = 256$ symbols. For these reasons, it is relevant to model the oscillator PN by a Gaussian distribution such that

$$\phi \sim \mathcal{N}(0, \sigma_\phi^2). \tag{3}$$

The PN variance σ_ϕ^2 is expressed in rad^2 and may be evaluated from the oscillator spectral characterization using $\sigma_\phi^2 = K_0/T$, where K_0 is the value of the spectral density of the oscillator white noise characteristic. By means of illustration, if we consider a channel bandwidth of $1/T = 1$ GHz, a measured spectral density $K_0 = -100$ dB entails a PN variance $\sigma_\phi^2 = 10^{-1}$. Interested readers may refer to [19] for the spectral characterization of a state-of-the-art sub-THz oscillator. For more details on the PN model selection, we refer the

[1]The presented results can also be exploited in channel bonding architectures.

[2]The propagation gain and phase shift of the channel are perfectly compensated.

reader to [10] or to [18]. The considered channel described by Eq. (1) and (3) is hereafter referred to as the GPN channel.

III. RECEIVER ALGORITHMS DESIGN

This section investigates the design of receiver algorithms for the GPN channel. First, we derive the *polar metric* and propose a low-complexity and efficient demodulation scheme. The decision rule for symbol detection, minimizing the SEP, and the corresponding soft-output demapper for coded systems are discussed. Second, we present a pilot-based channel estimation scheme in order to perform the optimum demodulation.

A. OPTIMUM DEMODULATION

1) SYMBOL DETECTION

Regarding symbol-by-symbol detection, the SEP is minimized by the maximum likelihood (ML) decision criterion [20] for equiprobable and independent transmitted symbols. The optimum detection decision rule is expressed upon $p(r|s)$ the channel likelihood function. With the considered channel in Eq. (1), it is appropriate to write the likelihood function as follows

$$p(r|s) = p(r_\rho, r_\theta | s_\rho, s_\theta), \tag{4}$$

and further to express (r_ρ, r_θ) from (s_ρ, s_θ). We denote the shifted noise $n \cdot e^{-j(s_\theta+\phi)}$ by n'. Since the complex noise is circularly symmetric, n and n' are identically distributed. It follows that the amplitude of the received symbol is given by

$$\begin{aligned} r_\rho &= \left|(s_\rho + n') \cdot e^{j(s_\theta+\phi)}\right|, \\ &= \sqrt{\left(s_\rho + \mathrm{Re}\,(n')\right)^2 + \mathrm{Im}\,(n')^2}, \\ &\simeq s_\rho + \mathrm{Re}\left(n'\right), \end{aligned} \tag{5}$$

and the phase by

$$\begin{aligned} r_\theta &= \arg\left((s_\rho + n') \cdot e^{j(s_\theta+\phi)}\right), \\ &= s_\theta + \phi + \arctan\left(\frac{\mathrm{Im}\left(n'\right)}{s_\rho + \mathrm{Re}\,(n')}\right), \\ &\simeq s_\theta + \phi + \frac{\mathrm{Im}\left(n'\right)}{s_\rho}. \end{aligned} \tag{6}$$

The two latter equations consider the transmission of non-zero symbols. If a zero symbol is sent, the channel in Eq. (1) is only corrupted by Gaussian noise. The first-order approximations in Eq. (5) and (6) are tight at high SNR. Since high data-rate applications are targeted in this work, it is reasonable to assume a high SNR in order to allow the use of high-order modulation schemes. Accordingly, we further pursue under a high SNR assumption. It is then straightforward from the channel and PN models in Eq. (1) and (3) that

$$\begin{aligned} (r_\rho - s_\rho) &\sim \mathcal{N}(0, \sigma_n^2), \\ (r_\theta - s_\theta) &\sim \mathcal{N}(0, \sigma_\phi^2 + \sigma_n^2/s_\rho^2). \end{aligned} \tag{7}$$

We conclude that the channel likelihood function can be expressed as a bivariate Gaussian distribution:

$$p(r|s) = \frac{\exp\left(-\frac{1}{2}\left(\frac{(r_\rho - s_\rho)^2}{\sigma_n^2} + \frac{(r_\theta - s_\theta)^2}{\sigma_\phi^2 + \sigma_n^2/s_\rho^2}\right)\right)}{2\pi\sqrt{\sigma_n^2(\sigma_\phi^2 + \sigma_n^2/s_\rho^2)}}. \tag{8}$$

This expression leads to the *ML premetric* decision rule originally derived in [21] and given by

$$\hat{s} = \arg\min_{s\in\mathcal{C}} \frac{(r_\rho - s_\rho)^2}{\sigma_n^2} + \frac{(r_\theta - s_\theta)^2}{\sigma_\phi^2 + \sigma_n^2/s_\rho^2} + \log\left(\sigma_\phi^2 + \frac{\sigma_n^2}{s_\rho^2}\right). \tag{9}$$

It has been shown in [21] and [22] that using the ML premetric leads to important performance gains in comparison to standard receivers based on the Euclidean distance – optimum for the complex AWGN channel. Due to its non-constant logarithmic term $\log(\sigma_\phi^2 + \frac{\sigma_n^2}{s_\rho^2})$, this decision rule might be complex to evaluate in practical systems. Further, this decision rule is entitled the ML premetric since it does not define a metric – neither symmetric nor sub-additive – and only a premetric. Exploiting a strong PN assumption, we have proposed in [22] the *polar metric* detection criterion. Its decision rule is given by

$$\hat{s} = \arg\min_{s\in\mathcal{C}} d_\gamma(r, s)^2, \tag{10}$$

where d_γ is the *polar metric* defined by

$$d_\gamma(r, s)^2 = (r_\rho - s_\rho)^2 + \frac{(r_\theta - s_\theta)^2}{\gamma^2}, \tag{11}$$

and $\gamma^2 = \sigma_\phi^2/\sigma_n^2 + 1/E_s$. The proposed detection criterion is the minimization of the distance related to the polar metric. The detected symbol is the closest constellation symbol to the received one. The demodulation therefore consists in a nearest neighbor search. It should be noted that this decision rule is a joint amplitude-phase detector. The polar metric is a weighted combination of the amplitude and phase of the received symbols. The decision rule is adapted to thermal and phase noise variances. When PN gets stronger, the detection relies more and more on the amplitude of received symbols rather than on the phase. Numerical simulations have demonstrated that exploiting a joint amplitude-phase detector rather than a Euclidean one yields valuable detection performance gains [21], [22]. In particular, the error floor in symbol detection caused by PN is significantly lowered by using an appropriate detection criterion. Results in [22] also demonstrate that the performance achieved by the polar metric, with a simpler expression, are identical to the one of the ML premetric at high SNR. One of the advantages of using the polar metric rather than the ML premetric is that the evaluation of distances to perform the detection is simpler to implement on practical systems. We will demonstrate in the following the benefits of the polar metric over the ML premetric. In the case of structured constellations, the polar metric greatly simplifies

the implementation of the receiver. With the polar metric, the symbol detection can be simplified as threshold comparisons and the evaluation of soft-bit values can be efficiently approximated with piecewise linear functions. These receiver complexity reductions are not possible with the ML premetric. In addition, the map d_γ verifies the algebraic properties of a metric. Subsequently, we pursue the analysis within the scope of complete metric spaces.

2) ANALYTICAL FRAMEWORK

We present here an original theoretical framework related to the polar metric. This framework enables us to draw a parallel between the GPN channel and the complex AWGN one. In particular, the proposed framework provides the analytical tools to design PN robust communication schemes, which will be used in the following section to optimize the signal constellation. It also gives tools to evaluate many literature proposals related to modulation design for PN channels.

Lemma 1: Let the complex number s be represented by its polar coordinates $(s_\rho, s_\theta) \in \mathbb{P} = [0, \infty) \times [-\pi, \pi]$. Then the space $\mathbb{P}^N$ - of sequences $\boldsymbol{s} = \{s_{\rho,k}, s_{\theta,k}\}_{1 \leq k \leq N}$ of N numbers in $\mathbb{P}$ - is a complete metric space when equipped with the metric $d_\gamma : \mathbb{P}^N \times \mathbb{P}^N \mapsto \mathbb{R}^+$ defined by

$$d_\gamma(\boldsymbol{x}, \boldsymbol{y})^2 = \sum_{k=1}^{N} \left((x_{\rho,k} - y_{\rho,k})^2 + \frac{(x_{\theta,k} - y_{\theta,k})^2}{\gamma^2} \right), \quad (12)$$

with $\gamma^2 \in \mathbb{R}_*^+$ for every $\boldsymbol{x}, \boldsymbol{y}$ vectors of $\mathbb{P}^N$.

Proof: It is sufficient to demonstrate that $\mathbb{P}^N$ is a closed subset of the complete metric space $(\mathbb{R}^{2N}, d_\gamma)$. First, it is clear that the map d_γ is a weighted Euclidean distance in $\mathbb{R}^{2N}$. It follows immediately that $(\mathbb{R}^{2N}, d_\gamma)$ is a complete metric space. Ultimately, the metric space $(\mathbb{P}^N, d_\gamma)$ is complete as $\mathbb{P}^N$ is clearly a closed subset of $\mathbb{R}^{2N}$. ■

In the following, p^2 denotes the metric space $(\mathbb{P}^N, d_\gamma)$. It results from Lemma 1 that p^2 is a complete metric space and therefore provides a valuable framework to design efficient algorithms for the GPN channel. For instance, the symbol detection based on nearest neighbor search in Eq. (11) can be efficiently implemented within p^2 using projections or sphere decoding. Furthermore, it should be noticed that a strong similarity exists between the GPN channel represented in the amplitude-phase domain and the complex AWGN channel in the in-phase quadrature (IQ) plane. This property can be highlighted by approximating, according to Eq. (7), the system model at high SNR as follows

$$(r_\rho, r_\theta) \simeq (s_\rho + n_\rho, s_\theta + n_\theta), \quad (13)$$

where n_ρ and n_θ follow Gaussian distributions. The radial noise n_ρ models the impact of thermal noise on the amplitude. By Eq. (7), we have $n_\rho \sim \mathcal{N}(0, \sigma_n^2)$. The angular noise n_θ models the contributions of both the PN and the thermal noise on the phase. In Eq. (7), the angular noise is given by $n_\theta \sim \mathcal{N}(0, \sigma_\phi^2 + \sigma_n^2/s_\rho^2)$. It should be recalled that the variance of the angular noise n_θ is function of (i) the amplitude of the sent symbol s_ρ (ii) the thermal noise variance σ_n^2 and (iii) the PN variance σ_ϕ^2. For the GPN channel, the noise on the amplitude and the noise on the phase are Gaussian and independently distributed. This property can also be observed on a complex AWGN channel in the IQ plane where the noise on the real part and the noise on the imaginary part are as well Gaussian and independently distributed. Accordingly, the space p^2 is entitled by analogy to the commonly used discrete signal space ℓ^2, the space of square-summable complex-valued sequences equipped with the Euclidean inner product.

Fig. 1 depicts the Voronoi regions – the ML decision regions – related to the Euclidean distance and the polar metric for a quadrature amplitude modulation (QAM) with 16 signal points. It illustrates the joint amplitude-phase feature of the polar metric detector. Furthermore, it should be emphasized that the polar metric in the amplitude-phase domain is defined as a weighted Euclidean distance as illustrated on Fig. 1(c). Altogether, the latter property along with Lemma 1 highlight the strong similarity between GPN and complex AWGN channels which will be used further to optimize the modulation scheme.

3) PROBABILISTIC DEMAPPER

It is of practical interest to consider the integration of a forward error correction (FEC) scheme in order to achieve a channel coding gain. Channel coding is usually combined with soft-decision decoding known to significantly improve the performance of channel decoders. We therefore propose in this paragraph to study the probabilistic demapper based upon the polar metric.

In practical communication systems, computing the exact values of the bit LLRs may be too complex. Therefore, close approximations of the bit LLRs are evaluated to be computed efficiently. We consider a bit-interleaved coded modulation (BICM) architecture. Let the symbol s map the binary word $\boldsymbol{b} = (b_1, \ldots, b_{\log_2(M)})$. Regarding the detection of bit b_i, the decision $\hat{b}_i$ minimizing the error probability is derived from the ML criterion [23]. We have

$$\hat{b}_i(r) = \begin{cases} 1, & \text{if } L_i(r) > 0 \\ 0, & \text{otherwise} \end{cases}, \quad (14)$$

where the LLR L_i of the bit b_i is given by

$$L_i(r) = \log \left(\frac{p(b_i = 1|r)}{p(b_i = 0|r)} \right). \quad (15)$$

The sign of L_i is used to infer the detection decision and its absolute value $|L_i|$ quantifies the reliability of this decision. Since transmitted symbols are equiprobable, we can express with Bayes' theorem the LLR as

$$L_i(r) = \log \left(\frac{\sum_{s_1 \in \mathcal{C}_1^i} p(r|s_1)}{\sum_{s_0 \in \mathcal{C}_0^i} p(r|s_0)} \right). \quad (16)$$

We adopt the notation $\mathcal{C}_\beta^i$ to describe the subset of the constellation symbols such that $b_i = \beta$. To simplify the computation of soft bit values, we derive sub-optimal LLRs expressions using the *log-sum* approximation: $\log(\sum_k x_k) \simeq \max_k \log(x_k)$.

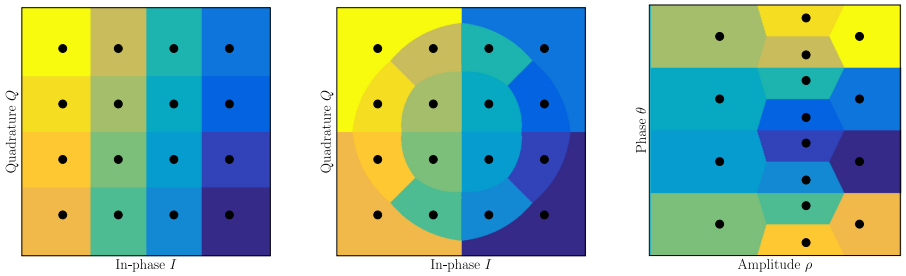

(a) Euclidean distance in ℓ^2 (b) Polar metric in ℓ^2 (c) Polar metric in p^2

FIG. 1. 16-QAM Voronoi regions.

This approximation is tight at high SNR and is commonly used in practical communications systems for conventional modulation schemes such as QAM [24]. It has been shown in [24] and in [25] that the log-sum approximation does not lead to any significant performance loss, even at low SNR. Subsequently, we obtain

$$L_i(r) \simeq \max_{s_1 \in \mathcal{C}_1^i} \log\left(p(r|s_1)\right) - \max_{s_0 \in \mathcal{C}_0^i} \log\left(p(r|s_0)\right). \qquad (17)$$

The channel decoding algorithms implemented in practical systems are not impacted by a normalization factor, for instance the *min-sum* decoder for low-density parity check (LDPC) codes. For this reason, the approximations of the LLRs are further expressed upon the polar metric introduced in Eq. (11) by

$$L_i(r) \simeq \min_{s_0 \in \mathcal{C}_0^i} d_\gamma(r, s_0)^2 - \min_{s_1 \in \mathcal{C}_1^i} d_\gamma(r, s_1)^2. \qquad (18)$$

The proposed bit LLR values in the latter expression can be easily evaluated. The computation of bit LLR values relies on the polar metric d_γ, and therefore, requires only the evaluation of few weighted Euclidean distances within p^2. In comparison, if the LLR computation is based on Eq. (16), the receiver is required to evaluate of several logarithmic terms as well as multiple sums of Gaussian functions of the received symbol. It should be further highlighted that such complexity reductions are not possible with the ML premetric as this decision rule implies several non-constant logarithmic terms. For this reason, the new soft-output demapper proposed in Eq. (18) allows significant complexity reductions of the receiver in comparison to state-of-the-art detectors [21]. It is worth mentioning that the expression in Eq. (18) of the bit LLRs remains valid if the propagation channel is considered by integrating a complex coefficient h to Eq. (1). The unique difference is that the variance of the thermal noise should be adapted.

Let us now evaluate the demodulation performance of coded systems over the GPN channel. The implemented FEC scheme is a LDPC code respecting the 5G new radio (5G-NR) specifications [26] with an input packet size of 1500 bytes, a coding rate of 0.8 and a *min-sum* decoder. LDPC codes demonstrate excellent performance with highly parallelizable decoder architectures. Therefore, they are considered

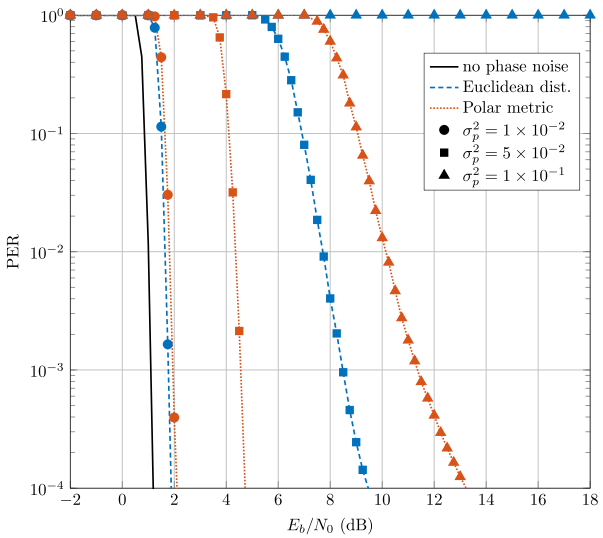

FIG. 2. Performance of a LDPC coded 16-QAM with LLR based on the Euclidean distance or on the polar metric for different PN variances σ_ϕ^2.

as a foremost solution for error-correcting codes in high-rate communication systems. Fig. 2 presents the packet error rate (PER) performance of a coded 16-QAM for different values of PN variance and demodulation schemes. Simulated PER have been obtained by Monte-Carlo simulations. Results show that important demodulation performance gains are achieved by the polar metric in comparison to the Euclidean detector. For low values of SNR and PN variance, the Euclidean detector performs slightly better than the polar metric (<0.1 dB). This minor performance loss results from the assumptions of a high SNR, in Eq. (5) and (6), and a strong PN used to derive the polar metric decision rule. When the PN variance gets stronger, the performance gain of the polar detector in comparison to the Euclidean one becomes significant – e.g. > 4 dB for $\sigma_\phi^2 = 5 \times 10^{-2}$. For strong PN variances, the PER of the receiver using the Euclidean distance is 1 for any SNR as the iterative decoder never converges. In contrast, the receiver based on polar metric demonstrates the waterfall feature of LDPC codes and can achieve low error rate communications. The presented PN variances: $\sigma_\phi^2 = 1 \times 10^{-2}$ rad^2, $\sigma_\phi^2 = 5 \times 10^{-2}$ rad^2 and

$\sigma_\phi^2 = 1 \times 10^{-1}$ rad^2 respectively correspond to an oscillator noise floor spectral density K_0 of -120 dB, -110 dB and -100 dB for a channel bandwidth of 1 GHz. Though more complex to compute, the demodulation algorithm based on ML premetric demonstrates identical performance to the one using polar metric one, and hence, is not presented. The proposed demodulation scheme has been assessed for QAM, yet remains valid for any modulation scheme. Ultimately, these results highlight that the proposed demodulation scheme based on the polar metric achieves important performance gains on the GPN channel with valuable complexity reductions of the receiver. Using channel statistics to properly represent the signal and optimize the communication algorithms is widely used. For instance, this is implemented in the orthogonal time frequency space (OTFS) waveform [27].

B. CHANNEL ESTIMATION

The previous subsection has shown that knowledge of the channel statistics may be used to improve the performance of the receiver. Therefore, estimations of thermal and PN variances: σ_n^2, σ_ϕ^2 are required. The PN variance σ_ϕ^2 results from the combination of two PN processes issued by the transmitter and the receiver oscillators, hence is not inherent to the receiver only. Estimation of σ_n^2 and σ_ϕ^2 may be realized by inserting N_p pilot symbols and by evaluating the appropriate estimators. The pilot symbols denoted $\boldsymbol{s} = (s_1, s_2, \ldots, s_{N_p})$ are known from the receiver and possibly distributed. The joint likelihood function of the N_p received pilot symbols $\boldsymbol{r} = (r_1, \ldots, r_{N_p})$ is given by

$$p_{N_p}(\boldsymbol{r}|\boldsymbol{s}, \sigma_n^2, \sigma_\phi^2) = \prod_{k=1}^{N_p} p(r_k|s_k, \sigma_n^2, \sigma_\phi^2). \tag{19}$$

It should be mentioned that here $k \in \{1, \ldots, N_p\}$ is the index of pilots symbols and may refer to non-consecutive received symbols. In the following we set pilot symbols to have a constant amplitude $\sqrt{E_s}$. The average symbol energy E_s is considered perfectly known as it can be estimated blindly through all sent symbols. It follows from the definition of the channel likelihood function in Eq. (8) that the ML estimators of σ_n^2 and σ_ϕ^2 are written as

$$\begin{aligned} \hat{\sigma}_n^2 &= \frac{1}{N_p} \sum_{k=1}^{N_p} (|r_k| - \sqrt{E_s})^2, \\ \hat{\sigma}_\phi^2 &= \frac{1}{N_p} \sum_{k=1}^{N_p} (/\, r_k - /\, s_k)^2 - \frac{\hat{\sigma}_n^2}{E_s}. \end{aligned} \tag{20}$$

We express these estimators as $\chi_{N_p}^2$ distributions to evaluate their biases and dispersions. That is

$$\begin{cases} \mathrm{E}\left[\hat{\sigma}_n^2\right] = \sigma_n^2, \\ \mathrm{V}\left[\hat{\sigma}_n^2\right] = \frac{2\sigma_n^4}{N_p}, \end{cases} \quad \begin{cases} \mathrm{E}\left[\hat{\sigma}_\phi^2\right] = \sigma_\phi^2, \\ \mathrm{V}\left[\hat{\sigma}_\phi^2\right] = \frac{2(\sigma_\phi^2 + \sigma_n^2/E_s)^2}{N_p} + \frac{2\sigma_n^4}{N_p E_s}. \end{cases} \tag{21}$$

It is clear that these estimators are unbiased. In addition, it is of practical interest to compare the proposed estimators to their Cramer-Rao lower bounds (CRLB) [28] since the regularity conditions are satisfied by the likelihood function in Eq. (8). The corresponding CRLBs are given by

$$\mathrm{V}\left[\hat{\sigma}_n^2\right] \geq \frac{2\sigma_n^4}{N_p}, \quad \mathrm{V}\left[\hat{\sigma}_\phi^2\right] \geq \frac{2(\sigma_\phi^2 + \sigma_n^2/E_s)^2}{N_p}. \tag{22}$$

It is shown that the thermal noise variance estimator achieves the CRLB. The estimator of the PN variance is tight to the CRLB but does not achieve it. Nevertheless, it is possible to demonstrate that the proposed estimators present the smallest mean square error among any unbiased estimators. It is immediate from Eq. (19), that the joint probability density function p_{N_p} belongs to the exponential family. Therefore, statistic $S = (\sum_{k=1}^{N_p}(|r_k| - \sqrt{E_s})^2,\ \sum_{k=1}^{N_p}(/\, r_k - /\, s_k)^2)$ is complete and sufficient for parameter $(\sigma_n^2, \sigma_\phi^2)$. We can conclude from the Lehman-Scheffé theorem that the proposed unbiased estimators $(\hat{\sigma}_n^2, \hat{\sigma}_\phi^2)$ defined upon S are the unique minimum-variance unbiased estimators of σ_n^2 and σ_ϕ^2.

The effect of a propagation channel with a single dominant path could be modeled by integrating a complex coefficient h to Eq. (1). Nonetheless, the estimation of the channel coefficient required for equalization is not carried out here. The necessary framework has been proposed such that the estimation of the channel complex coefficient is straightforward to derive.

IV. MODULATION SCHEME DESIGN

The previous section has investigated the design of receiver algorithms and thereby has unveiled valuable information on the GPN channel. We have previously considered a fixed modulation scheme to determine the optimum receiver. Nevertheless, it is clear that conventional modulation schemes such as QAM or phase-shift keying (PSK) are not suited to PN channels. This section is dedicated to the design of the modulation scheme for the GPN channel. A theoretical analysis is presented to construct PN robust constellations. Thereupon, we propose the Polar-QAM scheme. The constellation and the binary labeling of the Polar-QAM are jointly designed to improve communication performance on strong PN channels with a simple implementation. The performance analysis of the proposed modulation is pursued analytically and numerically to demonstrate the performance gains over conventional and state-of-the art schemes.

A. OPTIMUM CONSTELLATION FROM SPHERE PACKING

Let us investigate the problem of finding the constellation, i.e. the set of signal points in the complex plane, that minimizes the SEP for a given channel. The number of points is fixed to M and the constellation average energy is constrained to E_s. For a transmitted symbol, the SEP may be defined upon its complementary event, the probability of correct detection, as

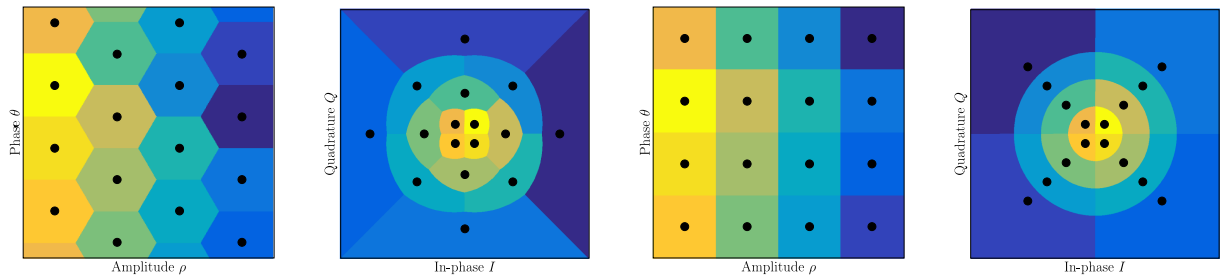

(a) Hexagonal polar-lattice in p^2 (b) Hexagonal polar-lattice in ℓ^2 (c) Rectangular polar-lattice in p^2 (d) Rectangular polar-lattice in ℓ^2

FIG. 3. Voronoi regions for the polar metric of polar-lattice based constellations with 16 signal points.

follows

$$P(E|s) = 1 - P(\hat{s} = s|s). \tag{23}$$

With regard to a detection rule defined upon the ML criterion, the probability of correct detection is proportional to the integration of the likelihood function over the Voronoi region of the symbol. That is

$$P(\hat{s} = s|s) \propto \int_{\mathcal{V}_s} p(r|s)dr, \tag{24}$$

where $\mathcal{V}_s$ is the Voronoi region of symbol s and $p(r|s)$ is the channel likelihood function. It follows that the larger the areas of the Voronoi regions, the smaller the error probability. This result is valid for any channel, yet let us consider the GPN channel. We are hence looking for the constellation that maximizes the areas of Voronoi regions defined by the polar metric. By way of illustration, it is clear on Fig. 1 that the QAM constellation does not maximize the areas of the Voronoi regions for the polar metric and is thus not optimal for the GPN channel. As previously stated, the proposed constellation in the literature lead to difficult implementations due to their lack of structure. We therefore investigate constellations defined upon lattices in the amplitude-phase plane. Since the ML detector in Eq. (10) describes a phase-amplitude detector, we study the optimal lattice-based constellation problem within p^2. It results that the noise distribution is circular[3] in p^2 for high SNR and strong PN scenarios. The modulation order and the average energy of the constellation being fixed, the problem of finding the lattice that maximizes the areas of the Voronoi regions can be regarded as finding the densest sphere packing in a two dimensional space. The well-known result of this problem gives that the highest density in the plane is achieved by the hexagonal lattice [29]. Subsequently, a constellation based upon a hexagonal structure is to maximize the areas of the Voronoi Regions [30], and thus, minimizes the SEP. Nevertheless, we consider hereafter the use of a rectangular polar-lattice to define a modulation scheme with the intention to ease the demapping implementation. For the purposes of illustration, Fig. 3 presents the IQ and amplitude-phase representations of the hexagonal and rectangular polar-lattice based constellation. Fig. 3 depicts the Voronoi regions, for the polar metric, of the constellations based on polar-lattice. We will show in the following paragraph that though a hexagonal lattice performs better in terms of error probability than a rectangular one, the performance gain is small and the complexity increase is significant. Therefore, the proposed Polar-QAM scheme relies on a rectangular polar-lattice.

We have previously highlighted the similarity between the GPN channel and the complex AWGN one. Thanks to the analytical framework described in this section, it follows that the derivation of the optimum lattice-based constellation for the GPN channel in the polar domain is highly similar to the one for the complex AWGN channel in the IQ plane – see [20]. Likewise, the optimal constellation for the complex AWGN channel relies on a hexagonal lattice in the IQ plane and is referred to as the hexagonal-QAM (HQAM). Though the HQAM demonstrates a performance gain in comparison to the QAM using a rectangular lattice [31], the rectangular QAM remains the most exploited modulation scheme for its simple implementation.

B. PERFORMANCE OF CONSTELLATIONS BASED ON POLAR-LATTICES

We discuss here the results of numerical simulation concerning the BER performance of the different constellations based on polar-lattices. The implemented symbol detection rule is the polar metric. The BER performance for different PN variances of the QAM and the polar-lattice based solutions are outlined in Fig. 4 with $M = 16$. First, we can remark that the optimized constellations are sub-optimal at low SNR. The previous analysis on the design of PN robust constellations is correct under a high SNR assumption. In the low SNR regime, the channel is dominated by thermal noise, even in the presence of strong PN, and in this case, conventional modulation schemes should be preferred. However, it is shown that the constellation of the QAM reaches an error floor due to PN which can be high for strong PN scenarios. Conversely constellation based on polar-lattice achieve significant performance gains and enable low error rate communications on strong PN channels. These results exhibit the performance gain of hexagonal lattice over the rectangular one, but at

[3]The noise is distribution is actually ellipsoidal in the amplitude-phase plane, yet is circular in p^2 with the axis scaling γ.

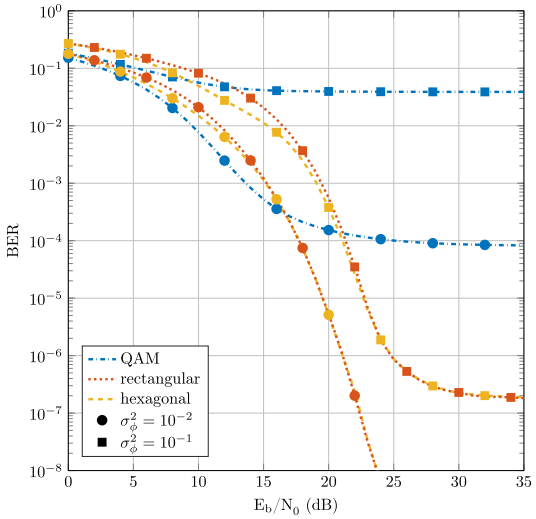

FIG. 4. BER performance of different constellations with $M = 16$ on the GPN channel.

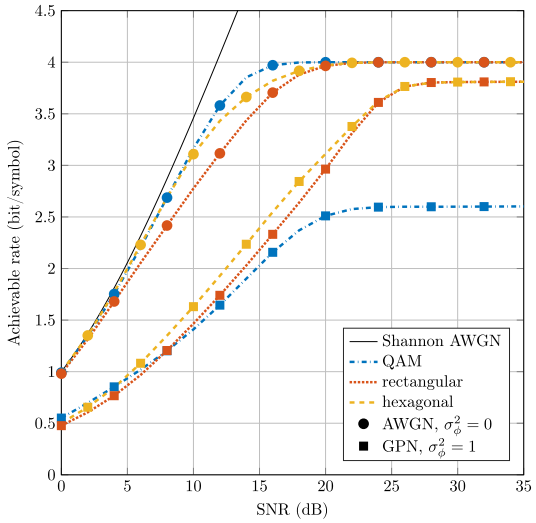

FIG. 5. Achievable rates in bit/symbol for different constellations and $M = 16$.

the detriment of a complexity increase of the demodulation algorithm.

The performance analysis can be improved by studying the achievable information rates (IR) related to the constellations. Fig. 5 compares the achievable rates of the different constellations for AWGN and GPN channels. The presented achievable IR have been obtained through Monte-Carlo simulations as described in [32]. Given a channel and a constellation, the achievable rate is evaluated by computing numerically the mutual information of the transmitted and received symbols. Our results demonstrate that the achievable rate of the QAM scheme is severely limited by PN. Therefore, we conclude that the optimization of the modulation scheme is essential to target high-rate communications on the GPN channel, and moreover, that constellations based on polar-lattices are a relevant solution.

In contrast to constellations obtained through numerical optimization [5], modulation schemes defined upon polar-lattices present an analytical signal points expression, and hence, result in a plain signal generation at the transmitter. Furthermore, the binary labeling regarding BICM architectures is trivial. In this case, the binary labeling in the polar domain is identical to the labeling in the IQ plane of a QAM for a rectangular lattice and respectively to a HQAM for a hexagonal lattice. The difference in implementation between the use of a hexagonal and a rectangular lattice to define the constellation is the following. It has been shown previously that the symbol detection is defined as a nearest neighbor search. As a result, this detection for a rectangular polar-lattice relies on simple threshold comparisons in the polar domain, as it can be observed on Fig. 3(c), which entails a simple demodulation algorithm. In addition, the bit LLR values related to a rectangular lattice and necessary to channel decoding can be approximated as piecewise linear functions in the amplitude-phase domain. These two complexity reductions at the receiver are enabled only with the use of a rectangular polar-lattice and not a hexagonal one. In conclusion, a constellation based on a hexagonal polar-lattice, in comparison to a rectangular one, leads to relatively small performance gains – see Figs. 4 and 5 – yet at the detriment of a more complex receiver. Therefore, we propose a modulation scheme based on a rectangular polar-lattice: the Polar-QAM.

It is interesting to mention that state-of-the-art approaches [5], [9], [33] on PN channels shape the constellations toward hexagonal and rectangular polar-lattices. For instance, the representation of the circular-QAM proposed in [33] in the amplitude-phase domain is close to a hexagonal lattice. Further, it has been shown in [33] that the circular-QAM realizes, in comparison to a conventional QAM, performance gains on PN channels. Similarly, it is worth studying the Gray-APSK proposed in [34] to provide a shaping gain for satellite communications. Signal points of the Gray-APSK represented in the amplitude-phase domain nearly describe a rectangular lattice, the amplitudes of signal points are non-linearly distributed though. Thanks to the presented analysis, we can conclude that such modulation scheme should provide valuable performance gains on PN channels.

Eventually, the following remark should be pointed out. We have presented here a theoretical analysis based on the signal decomposition in the amplitude-phase domain to optimize the modulation scheme for the GPN channel. This original analysis provides a valuable theoretical framework to design PN robust communication schemes and also to evaluate many of the literature proposals.

C. POLAR-QAM

The proposed Polar-QAM is defined by the constellation $\mathcal{C}$ illustrated in Fig. 6. With $m, n \in \mathbb{N}$ and $m \geq n$, the constellation $\mathcal{C}$ is a set of $M = 2^m$ complex points placed on $\Gamma = 2^n \in \{1, 2, 4, \ldots, M\}$ concentric circles, i.e. amplitude levels.

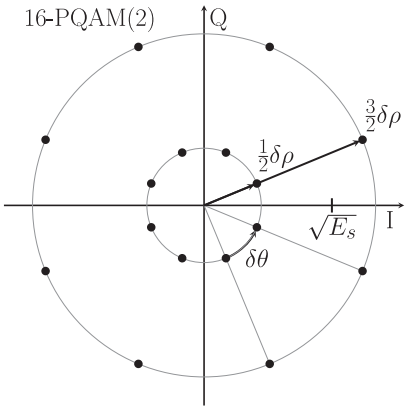

FIG. 6. Illustration of a 16-PQAM(2) in the complex plane.

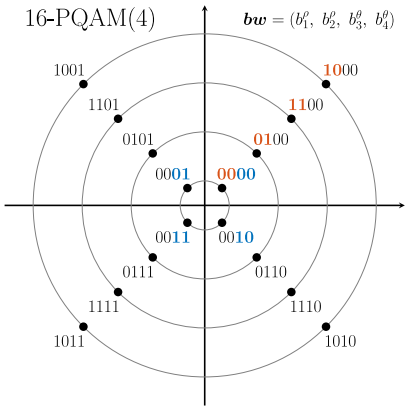

FIG. 7. Binary labeling of a 16-PQAM(4).

The average energy of the constellation is denoted E_s. Each of the Γ circles contains M/Γ signal points. Correspondingly, the *minimum angular distance* $\delta\theta$ between two symbols is

$$\delta\theta = \frac{2\pi\Gamma}{M}. \tag{25}$$

The phase shift θ_p of the p-th symbol on a circle is described by $\theta_p = \frac{\delta\theta}{2}(2p-1)$. Likewise, the amplitude ρ_q of the q-th circle ρ_q is defined by $\rho_q = \frac{\delta_\rho}{2}(2q-1)$ where $\delta\rho$ is the *minimal radial distance*. It results from this definition of the amplitudes of signal points and from the average symbol energy E_s that the minimal radial distance $\delta\rho$ is given by

$$\frac{\delta\rho}{\sqrt{E_s}} = \sqrt{\frac{12}{4\Gamma^2-1}}. \tag{26}$$

Then, any PQAM constellation can be entirely defined by two parameters M and Γ respectively the modulation order and shape. Therefore, we use the notation M-PQAM(Γ) to described the constellation

$$\mathcal{C} = \left\{ \frac{\delta\rho}{2}(2q-1)\cdot\exp\left(j\cdot\frac{\delta\theta}{2}(2p-1)\right) \right. \\ \left. \mid 1\le q\le\Gamma, 1\le p\le M/\Gamma \right\} \tag{27}$$

One may remark that some particular cases of the PQAM fall into known modulations: a M-PQAM($M/2$) describes an amplitude-shift keying while a M-PQAM(1) is a PSK. The PQAM is a structured definition of an APSK constellation. For the demodulation of the PQAM on the GPN channel, it is relevant to use the proposed detection scheme based on the polar metric. When this demodulation scheme is used, the symbol detection for the PQAM can be implemented with a simple threshold detection in the amplitude-phase domain.

Nonetheless, the PQAM is not only defined by its constellation but also by its binary labeling. For a given channel, optimizing the symbol mapping in order to minimize the bit error rate (BER) is not trivial and induces a high complexity – *cf.* binary switching algorithm [35]. Thanks to the regular structure of the PQAM, an efficient binary labeling can be proposed in order to achieve robustness and simple demodulation. In a 2^m-ary modulation system, every m bits form a binary word $\boldsymbol{b}\in\{0,1\}^m$, which is modulated to a symbol $s\in\mathcal{C}$ under a mapping rule called constellation labeling μ,

$$\mu : \{0,1\}^m \to \mathcal{C}. \tag{28}$$

To minimize the bit error probability, the mapping rule must implement a Gray code. Namely, a Gray code mapping consists in labeling the M points with binary words of length $m=\log_2(M)$ such that the Hamming distance between two nearest points is equal to 1. Subsequently, incorrectly estimating a symbol by one of its nearest neighbors leads to a single bit error. In the case of a M-PQAM(Γ), any binary words $\boldsymbol{b}\in\{0,1\}^{\log_2(M)}$ mapped to a symbol s may be expressed as

$$\boldsymbol{b} = (b_1^\rho,\ldots,b_{\log_2(\Gamma)}^\rho, b_{\log_2(\Gamma)+1}^\theta,\ldots,b_{\log_2(M)}^\theta) \tag{29}$$

where $\log_2(\Gamma)$ bits are encoded by the amplitude level s_ρ of s, and $\log_2(M/\Gamma)$ bits are encoded by the phase s_θ of s. Therefore, the mapping rule μ may be subdivided into two uni-dimensional rules μ_ρ and μ_θ:

$$\begin{aligned} \mu_\rho &: \{0,1\}^{\log_2(\Gamma)} \to s_\rho, \\ \mu_\theta &: \{0,1\}^{\log_2(M/\Gamma)} \to s_\theta. \end{aligned} \tag{30}$$

Uni-dimensional mapping of signal points respecting a Gray code is straightforward and a well-known result. It is worth mentioning that the PQAM constellation has been designed to achieve such efficient binary labeling. Fig. 7 depicts the binary labeling for a 16-PQAM(4). Conversely, optimized constellations of the literature present no particular structure and lead to complex labeling and poor performance in terms of BER. Besides, the binary labeling of the Polar-QAM allows low-complexity evaluation of the bit LLR. When the PQAM is used with the proposed soft-output demapper based on the polar metric, the soft-bit values can be efficiently approximated with piecewise linear functions. The piecewise linear approximations of the LLR of the $\log_2(\Gamma)$ bits related to the amplitude level present similar expressions to the ones of a QAM constellation, see [36]. While for the $\log_2(M/\Gamma)$ bits encoded on the phase, approximations are similar to a PSK [37].

The evaluation of the bit LLRs based on piecewise linear functions is an important complexity reduction of the receiver. This complexity reduction highlights the benefits of using the PQAM and the proposed demodulation scheme over state-of-the-art solutions, based on numerically optimized constellations. It also emphasizes the relevance of jointly optimizing the modulation and demodulation schemes.

D. THEORETICAL PERFORMANCE ANALYSIS

Let us evaluate the detection error probability $P(E)$ expressed by

$$P(E) = \frac{1}{M}\sum_{s\in\mathcal{C}} P(\hat{s}\neq s|s) = \frac{1}{M}\sum_{s\in\mathcal{C}} (1 - P(\hat{s} = s|s)). \tag{31}$$

By definition of the PQAM, we can approximate the probability of correct detection as follows

$$P(\hat{s} = s|s) \simeq P\left(-\frac{\delta\rho}{2} < (s_\rho - r_\rho) < \frac{\delta\rho}{2}\right) \times P\left(-\frac{\delta\theta}{2} < (s_\theta - r_\theta) < \frac{\delta\theta}{2}\right). \tag{32}$$

It follows from the expression of the channel likelihood function that the detection error probability is given by

$$P(E) \simeq 2Q\left(\frac{\delta\rho}{2\sigma_n}\right) + 2Q\left(\frac{\delta\theta}{2\sqrt{\sigma_\phi^2 + \sigma_n^2/E_s}}\right). \tag{33}$$

The latter approximation holds for high SNR and corresponds to the widely used assumption that errors occur on the nearest neighbors of the sent symbol. To simplify the closed form expression in Eq. (32), it is assumed that the average detection errors on the phase of symbols occur for an amplitude of $\sqrt{E_s}$ which is slightly optimistic – see Section IV-E. Since the binary labeling implements a Gray code mapping and under the nearest neighbors error assumption, the bit error probability P_{be} may be derived from the symbol detection error probability as

$$P_{be} = \frac{P(E)}{\log_2(M)}. \tag{34}$$

Let us replace $\delta\rho$ and $\delta\theta$ by their definitions in Eq. (25) and (26) to express the BER as a function of E_b/N_0, σ_ϕ^2, M and Γ. Hereafter, it is assumed that $T = 1$ which results in no loss of generality. The average bit energy $E_b = E_s/\log 2(M)$ and the noise power spectral density $N_0 = 2\sigma_n^2$. Eventually, the BER of a M-PQAM(Γ) can be approximated by the following closed-formed expression

$$P_{be} \simeq \frac{2}{\log_2(M)}\left[Q\left(\sqrt{\frac{6\cdot\log_2(M)\cdot E_b/N_0}{4\Gamma^2-1}}\right) + Q\left(\frac{\pi\Gamma}{M\sqrt{\sigma_\phi^2 + \frac{1}{E_b/N_0}\frac{1}{2\cdot\log_2(M)}}}\right)\right] \tag{35}$$

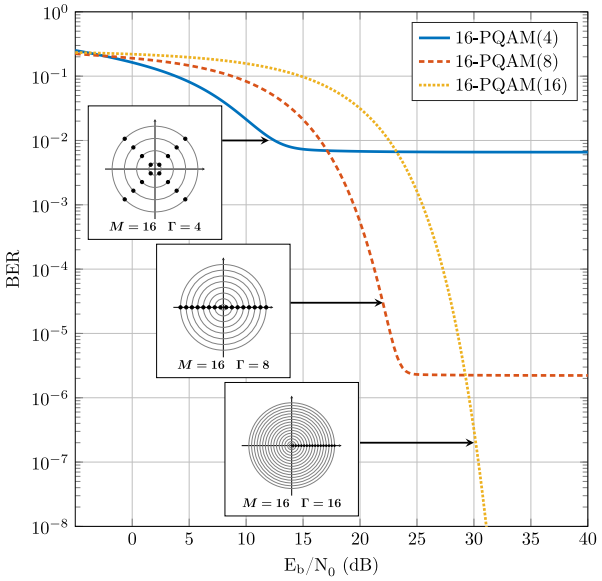

FIG. 8. Analytical performance of a 16-PQAM(Γ) for modulation shape $\Gamma \in \{4, 8, 16\}$ with PN variance $\sigma_\phi^2 = 1.25 \times 10^{-1}$.

In the BER expression, the two terms in the addition should be interpreted differently. The first term expresses the probability of misestimating the amplitude level of the received symbol whereas the second one the phase. Fig. 8 outlines the analytical BER performance of a 16-PQAM(Γ) for $\Gamma \in \{4, 8, 16\}$ and their respective constellations. As depicted in Fig. 8, the BER reaches an error floor when E_b/N_0 tends to infinity due to PN. This error floor is given by

$$\lim_{E_b/N_0\to\infty} P_{be} = \frac{2}{\log_2(M)} Q\left(\frac{\pi\Gamma}{M\sigma_\phi}\right). \tag{36}$$

It is shown in Fig. 8 and in Eq. (36) that the smaller Γ, the higher the error floor. For a PN channel, the error floor of a constellation is caused by several signal points using the same amplitude level and can be lowered by increasing the minimum angular distance. In brief, a large number of amplitude levels Γ entails a low error floor, yet attained at a higher E_b/N_0.

With regard to the RF power-amplifiers, directly related to the energy consumption of transmitters, the peak-to-average power ratio (PAPR) is a key performance indicator for any communication system. In the context of the Polar-QAM, the PAPR is given by

$$\frac{\max\limits_{s\in\mathcal{C}} |s|^2}{E_s} = 3\cdot\frac{2\Gamma-1}{2\Gamma+1}. \tag{37}$$

It can be noticed that the PAPR is a strictly increasing function of the number of amplitude levels Γ and is not function of the modulation order M. As previously mentioned increasing Γ does improve the PN robustness at the detriment of a higher PAPR. Finally, the closed-form expressions of the BER and the PAPR of the Polar-QAM provide new and valuable results

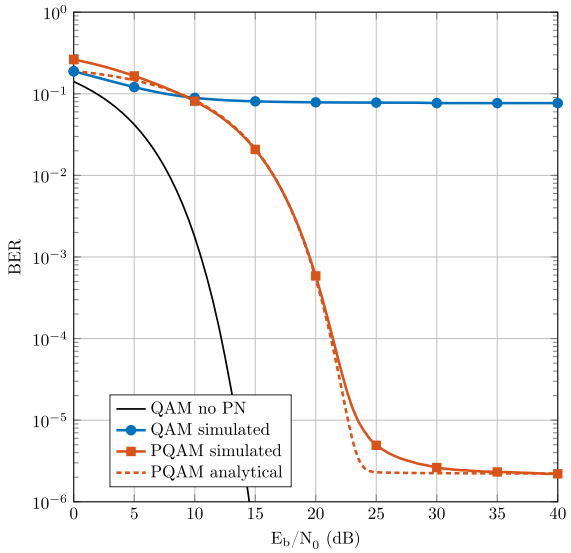

FIG. 9. 16-QAM and 16-PQAM(8) performance with PN variance $\sigma_\phi^2 = 1.25 \times 10^{-1}$.

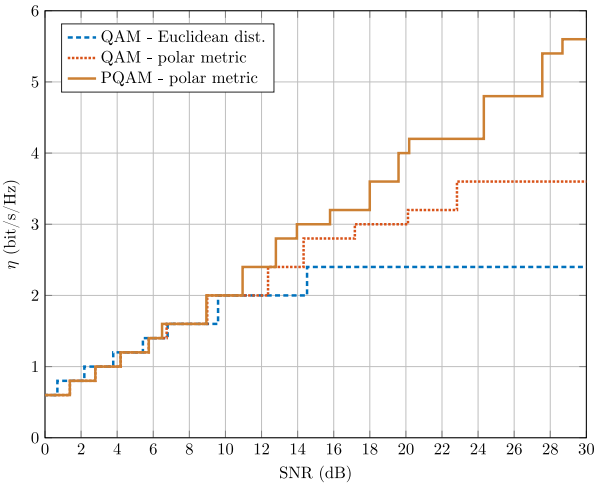

FIG. 10. Achievable rate in bit/symbol of the QAM and PQAM schemes with a LDPC code and PN variance $\sigma_\phi^2 = 10^{-1}$.

for the specification and analysis of future systems. The theoretical analysis of such important performance metrics is not possible for the numerically optimized constellations of [5] or the state-of-the-art modulation proposed in [9]. This further motivates the use of a structured constellation, and also, the joint optimization of the modulation and demodulation schemes.

E. NUMERICAL SIMULATIONS RESULTS

The results of numerical simulations for uncoded systems are presented in Fig. 9. The BER performance of the QAM and PQAM are compared for $M = 16$ and $\sigma_\phi^2 = 1.25 \times 10^{-1}$. The demodulation with the polar metric detector is implemented. Results demonstrate the performance gain achieved by the PQAM constellation over a conventional QAM on a strong GPN channel. The QAM constellation presents a high error floor which results from the low angular distance between its signal points. Nonetheless, it is worth mentioning that this performance gain is achieved to the detriment of the PAPR. A 16-QAM presents a PAPR of 2.55 dB while the 16-PQAM(8) exhibits a 4.23 dB PAPR. It is also illustrated that the analytical expression of the BER for a PQAM is tight to the simulation results. Nevertheless, the optimistic consideration made in Eq. (32) is to explain the slight difference between the analytical expression and the simulation results.

Fig. 10 presents the results of numerical simulation for coded systems. It outlines the achievable rate in bit/symbol for $\sigma_\phi^2 = 10^{-1}$ and a LDPC code. Three modulation/demodulation schemes are considered: QAM with Euclidean detector, QAM with polar detector and PQAM with polar detector. The FEC scheme is based on the 5G-NR LDPC and is implemented with an input packet size of 1500 bytes and a coding rate ranging from 0.3 to 0.9. The communication performance has been characterized to determine the best set of parameters: coding rate, modulation order M and modulation shape Γ given the SNR, the PN variance while targeting a PER of 10^{-2}. A PER of 10^{-2} is targeted for numerical evaluations. This quality of service gives reliable transmission with low throughput penalty when automatic repeat request scheme is implemented. It avoids the design of low error floor and reliable FEC scheme. This level of PER is widely considered in modern wireless communication standards [26]. The PN variance $\sigma_\phi^2 = 10^{-1}$ rad^2 corresponds to an oscillator spectral density K_0 of -100 dB for a bandwidth of 1 GHz. These simulation results emphasize the benefits of using optimized modulation and demodulation schemes to implement high-rate communication systems impaired by PN. In the low SNR regime, the optimized schemes exhibit some performance losses on the achievable rate. These losses result from the high-SNR and strong PN assumptions made to derive the polar metric and to construct the PQAM. These results confirm that at low SNR, and even with strong PN, conventional modulation schemes such as QAM should be used. Furthermore, it should be mentioned that the probabilistic bit values derived for the PQAM upon the polar metric decision rule present non-uniform protections. With regard to the SNR and PN variance, the bits mapped on the phase and on the amplitude experience different levels of protection. A joint optimization of the modulation and the channel coding (e.g. similar to multi-level coding techniques) could exploit the latter property to further enhance the demodulation performance and increase the achievable rate.

F. COMPARATIVE STUDIES

1) ASYMPTOTIC PERFORMANCE

Table 1 presents the asymptotic SEP performance of different constellations from prior work for $\sigma_\phi^2 = 10^{-2}$. This table is extracted from [5] and has been completed with our proposition. The error floors of PQAM have been obtained with the closed form expression given in Eq. (36). It should be

TABLE 1. Comparison of Error Floors for Different Constellations and $\sigma_\phi^2 = 10^{-2}$

Constellation	$\text{SEP}_{E_b/N_0 \to +\infty}$
16-PSK	5.0×10^{-2}
16-QAM	3.5×10^{-4}
Foschini *et al.* [6]	2.2×10^{-4}
16-PQAM(4)	4.0×10^{-15}
16-PQAM(8)	1.3×10^{-55}
Krishnan *et al.* [5]	0
16-PQAM(16)	0

remarked that conventional modulation schemes such as PSK or QAM demonstrate high error floors. In contrast, optimized constellations does not exhibit any error floor. As aforementioned in Section IV-D, the larger the minimum angular distance of a constellation, the lower the error floor. It is hence shown that low error floor communications can be achieved by using a large number of amplitude levels to define the constellation.

2) STATE-OF-THE ART CONSTELLATION

The definition of the Polar-QAM is close to the one of the Gray-APSK, proposed in [34] to provide a shaping gain for satellite communications and not to achieve PN robustness. Both modulation schemes use structured APSK and two independent Gray mapping on the phase and on the amplitude, and hence, demonstrate similar performance. The difference between these constellations is that the amplitudes of Gray-APSK signal points are non-linear. We have proposed the Polar-QAM and derived its analytical and numerical performance analysis in the context of PN channels. For this reason, we compare in this paragraph the performance of the proposed solution to the one of the, most recent, state-of-the-art solution proposed in [9] on constellation optimization for the GPN channel: the *spiral* constellation. Nonetheless, interested readers may refer to [9] which evaluates the performance of the Gray-APSK. Fig. 11 compares the SEP performance of the PQAM and the spiral constellation for $M = 64$ and $\sigma_\phi^2 = 10^{-1}$ demodulated with a polar metric receiver. It is shown that the spiral constellation demonstrates a performance gain in comparison to the PQAM at the expense of a transceiver complexity increase. The spiral constellation presents a semi-analytical description: the modulation points are defined with a closed-form expression upon an optimized modulation shape parameter $f_s \in \mathbb{R}_{\geq 0}$. For each SNR point, the spiral constellation requires the optimization of the parameter f_s through important Monte-Carlo simulations to maximize the achievable information rate of the modulation. Conversely to this, the modulation shape parameter Γ of the Polar-QAM belongs to a small finite set; and therefore, adapting the modulation scheme to the channel is straightforward. Though a simple and efficient symbol detection rule is proposed in [9], the binary labeling of the spiral constellation entails a complex LLR evaluation which cannot be efficiently approximated.

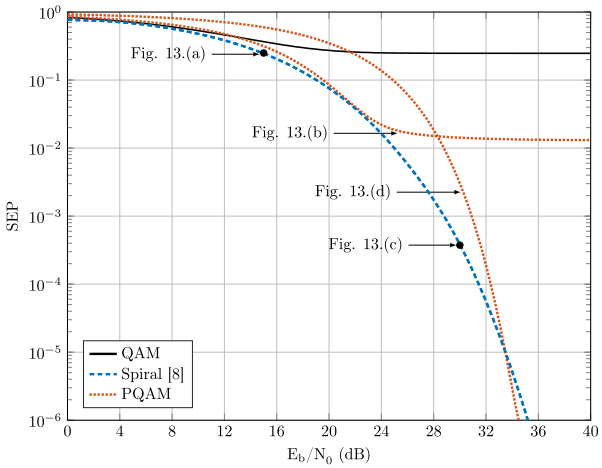

FIG. 11. Comparison of PQAM to the spiral constellation [9] with $M = 64$ and $\sigma_\phi^2 = 10^{-1}$.

Fig. 11 precisely illustrates the benefits of the proposed solution: near-optimal performance are achieved with a simple implementation. By way of illustration, Fig. 12 presents the Polar-QAM and spiral constellations in the IQ plane and in the amplitude-phase domain. It can be observed on Fig. 12(e) that the definition of the spiral constellation is actually closed to a hexagonal polar-lattice in the amplitude-phase domain. The Polar-QAM and the spiral constellations demonstrate similar PAPR values. For the spiral constellation optimized for $E_b/N_0 = 30$ dB the PAPR is 4.66 dB while the PAPR of the 64-PQAM(32) is 4.64 dB.

3) COMPLEXITY OF IMPLEMENTATION

It is clear that numerically optimized constellations, and more generally speaking generalized APSK modulations, are difficult to demodulate due to the complex nature of the Voronoi regions. Conversely, using the proposed Polar-QAM and polar metric detector, the symbol detection can be implemented with a simple Cartesian-to-polar transform followed by an independent component processing with threshold detection. Considering a soft-decision decoding, with a soft-output demapper, the Polar-QAM is even more beneficial. On one hand, non-structured constellations leads to multi-dimensional processing involving all signal points. This leads to a wide literature to reduce decoder complexity, see [38] or [39]. On the other hand, with the Polar-QAM, the commonly used log-sum approximation – e.g. widely considered for QAM demapping – can be implemented after the Cartesian-to-polar transform. In addition, the binary labeling and linear structure of the Polar-QAM enables efficient approximations of the bit LLR values with piecewise linear functions, similar to the ones presented in [36] and in [37], and therefore leads to a significant complexity reduction of the decoder. This is a important benefit of using the PQAM and

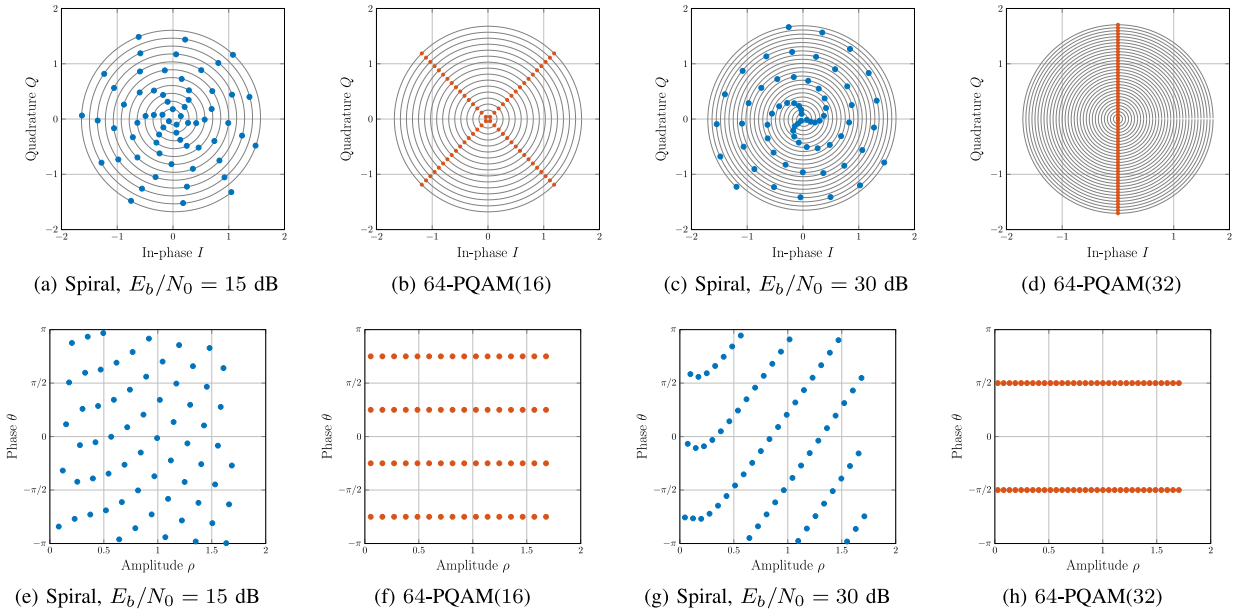

(a) Spiral, $E_b/N_0 = 15$ dB (b) 64-PQAM(16) (c) Spiral, $E_b/N_0 = 30$ dB (d) 64-PQAM(32)

(e) Spiral, $E_b/N_0 = 15$ dB (f) 64-PQAM(16) (g) Spiral, $E_b/N_0 = 30$ dB (h) 64-PQAM(32)

FIG. 12. Spiral and PQAM constellations in ℓ^2 (first row) and in p^2 (second row).

the polar metric. In comparison to state-of-the-art techniques, it offers significant complexity reductions of the receiver.

V. APPLICATIONS & PERSPECTIVES

The aim of this section is to highlight potential applications and perspectives the proposed schemes. First, sub-THz applications based on channel bonding may use non-contiguous bands in a wide frequency range leading to significant differences in the performance of oscillators [2]. Accordingly, we propose a new link adaptation scheme to maintain robustness by setting the Polar-QAM parameters with regard to the SNR and PN variance. Second, the memoryless model of PN may be considered as an optimistic assumption. Therefore, we present a differential version of the PQAM which is more robust to the cumulative PN. Before concluding the paper, some perspectives to this work are outlined.

A. LINK ADAPTATION

In order to maximize the spectral efficiency, practical communication systems implement adaptive modulation schemes. Namely, the modulation order is set with regard to the quality of the channel. In particular, a link adaptation scheme is highly valuable for sub-THz communications. Regarding contemplated applications for terrestrial and vehicular networks [4], a base station is to address several users' equipment with different qualities, and thus, different SNR and PN levels. Moreover, for channel bonding systems, the aggregated spectrum may be wide enough to exhibit significant differences between oscillators performance in higher and lower frequencies. In the case of the Polar-QAM, we propose a new link adaptation strategy which is developed beyond adjusting the modulation order M of conventional techniques, by also adapting the modulation shape with parameter Γ. In particular, the introduced

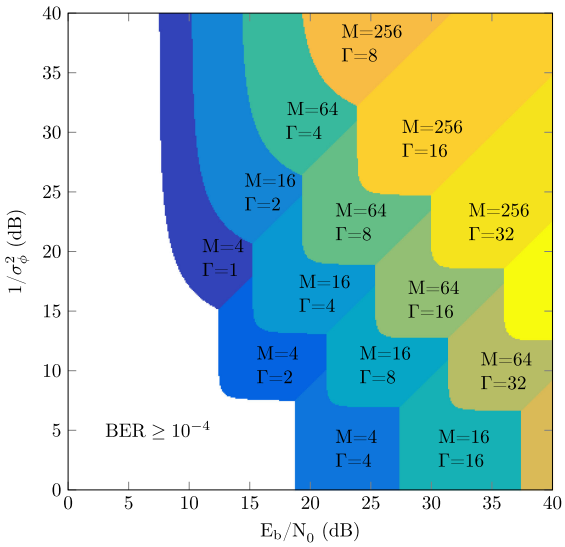

FIG. 13. PQAM parameters M and Γ with the highest spectral efficiency such that BER< 10^{-4}.

theoretical analysis of the performance of the Polar-QAM is valuable for the link adaptation. We can use the analytical expression of the BER in Eq. (35) to determine the best set of parameters (M, Γ) to achieve the highest spectral efficiency while maintaining the BER below a fixed threshold. Fig. 13 presents the PQAM parameters M and Γ for a given PN variance σ_ϕ^2 and E_b/N_0 such that the spectral efficiency is maximized and the BER remains inferior to 10^{-4}. This link adaptation strategy requires a channel estimation scheme which has been previously introduced in Section III-B. It should be emphasized that the Polar-QAM enables a simple

link adaption strategy. In contrast to state-of-the-art solutions, the modulation order and shape parameters (M, Γ) belong to small finite sets, and therefore, adapting the modulation scheme to the channel conditions is straightforward.

B. BEYOND MEMORYLESS PHASE NOISE

The phase shift induced by the propagation channel must be estimated and then corrected. Generally speaking, pilot-based estimation schemes are considered and lead to a spectral efficiency loss. Moreover, the oscillator at the receiver may not be synchronized to the carrier frequency of the transmitter resulting in a carrier frequency offset (CFO). If the CFO is not perfectly estimated and compensated, then a residual frequency synchronization error corrupts received symbols with a cumulative phase error. This phase error is increasing between reference pilots and phase corrections, and thus, can be modeled as cumulative PN. Besides, it has been stated in Section II-B that oscillator PN also demonstrates a cumulative nature. For these reasons, the cumulative PN in certain systems might not be negligible or not perfectly compensated using reference signals. These impairments affecting practical systems lead to performance degradation and motivate the use of a differential modulation. It should be mentioned that the use of differential M-QAM with $M > 4$ is not simple and remains challenging to design. In contrast to conventional solutions or state-of-the-art constellations, the proposed modulation scheme has the advantage of being straightforwardly compatible with a differential scheme. We denote DPQAM the Differential implementation of the PQAM. The information encoded upon the amplitude of symbols remains identical whereas the phase information is encoded in the relative phase difference between two symbols. Subsequently, the DPQAM is not subject to the initial phase shift of the channel. We propose the DPQAM to provide a high-order modulation scheme with an improved robustness to the cumulative PN and residual CFO. The performance analysis of the DPQAM has been pursued but exceeds the scope of this study and is to be released in a further work. Nevertheless, one may refer to our previous work [40] which assessed analytically and numerically the performance degradation due to cumulative PN for phase modulated signals.

C. PERSPECTIVES

We have presented in this paper the main transmission schemes to realize robust communications impaired by PN. However, many algorithms regarding practical communications are yet to be addressed. In particular, the synchronization between the transmitter and the receiver in the presence of strong PN is challenging. Time and frequency synchronization errors lead respectively to inter-symbols interference and CFO. Synchronization errors need to be compensated in order to limit the resulting performance degradation. For this reason, dedicated synchronization techniques should be designed for systems impaired by strong PN. This topic is of important practical interest and remains to be investigated. The design of dedicated RF architectures is also interesting to investigate. Since symbols of the Polar-QAM constellation is entirely defined by their phase and amplitude, a conventional IQ transmitter RF architecture may not be relevant and could be replaced by a *polar RF transmitter* – a widely known technique, see [41]. In this paper, we have considered an IQ receiver RF chain and have shown that the optimal demodulation uses polar coordinates. It is hence legitimate to contemplate the benefit of a *polar RF receiver* [42] which outputs directly the phase and amplitude of received symbols. Furthermore, it is of practical interest to study the impact of quantization. Contrary to usual IQ schemes in which the quantization strategy is the same on the two signal paths, the use of asymmetric strategies could be relevant for polar RF receivers, especially in the context of a GPN channel. In this paper, different signal processing techniques have been discussed to mitigate the performance degradation due to PN. It should also be mentioned that on-going research works are dedicated to the design of sub-THz oscillators with low PN characteristics [19].

VI. CONCLUSION

We have investigated the design of robust communications impaired by strong PN for future sub-THz applications. We have developed a pragmatic approach supported by a theoretical framework. This problem has been addressed in three steps: the characterization of the PN channel, the design of receiver algorithms, and the optimization of the modulation scheme. First, we have introduced the system model for sub-THz communication systems. A LoS propagation channel has been considered and the oscillator PN has been described by a Gaussian process. Second, we have addressed the design of the optimum demodulation scheme for the GPN channel. The polar metric has been derived as a symbol detection scheme minimizing the error probability. We have also proposed a low-complexity implementation of the soft-output demapper using the polar metric for probabilistic channel decoding. In contrast to state-of-the-art detectors, the proposed soft-output demapper allows a simple evaluation of soft bit values. Simulation results show that significant demodulation performance gains are achieved by using the polar metric in comparison to standard detectors. Third, we have studied the optimization of the modulation scheme for the GPN channel. A mathematical framework, based on a signal decomposition in polar coordinates, has been presented to design robust constellations and also to evaluate state-of-the-art solutions. It has been shown that a constellation defined upon a lattice in the amplitude-phase domain is robust to PN and leads to a low-complexity implementation. Thereupon, we have proposed the Polar-QAM scheme. The constellation and the binary labeling of the Polar-QAM are jointly designed to enhance the system performance with a low-complexity implementation. We have compared the proposed modulation to conventional and state-of-the-art solutions on different performance metrics such as the PAPR, the BER, or the achievable rate. Our results highlight the important performance gains realized by the Polar-QAM in comparison to conventional schemes. In

contrast to state-of-the-art optimized constellations, the advantage of the proposed solution is that near-optimal performance is achieved with significant complexity reductions of the transceiver. To conclude, we have shown in this work that optimizing the communication schemes is essential to realize high rate communications on practical systems impaired by strong PN. Accordingly, the proposed schemes offer valuable low-complexity solutions for future sub-THz systems.

REFERENCES

[1] T. S. Rappaport *et al.*, "Wireless communications and applications above 100 GHz: Opportunities and challenges for 6G and beyond," *IEEE Access*, vol. 7, pp. 78 729–78 757, 2019.

[2] J.-B. Doré *et al.*, "Above-90 GHz spectrum and single-carrier waveform as enablers for efficient Tbit/s wireless communications," in *Proc. 25th Int. Conf. Telecommun.*, Jun. 2018, pp. 274–278, doi: 10.1109/ICT.2018.8464918.

[3] S. Mumtaz, J. Jornet, J. Aulin, W. Gerstacker, X. Dong, and B. Ai, "Terahertz communication for vehicular networks," *IEEE Trans. Veh. Technol.*, vol. 66, no. 7, pp. 5617–5625, Jul. 2017.

[4] H. Elayan, O. Amin, B. Shihada, R. M. Shubair, and M. Alouini, "Terahertz band: The last piece of RF spectrum puzzle for communication systems," *IEEE Open J. Commun. Soc.*, vol. 1, pp. 1–32, 2020.

[5] R. Krishnan, A. G. I. Amat, T. Eriksson, and G. Colavolpe, "Constellation optimization in the presence of strong phase noise," *IEEE Trans. Commun.*, vol. 61, no. 12, pp. 5056–5066, Dec. 2013.

[6] G. J. Foschini, R. D. Gitlin, and S. B. Weinstein, "On the selection of a two-dimensional signal constellation in the presence of phase jitter and gaussian noise," *Bell Syst. Tech. J.*, vol. 52, no. 6, pp. 927–965, Jul. 1973.

[7] F. Kayhan and G. Montorsi, "Constellation design for channels affected by phase noise," in *Proc. IEEE Int. Conf. Commun.*, Jun. 2013, pp. 3154–3158.

[8] C. Hager, A. G. I. Amat, A. Alvarado, and E. Agrell, "Design of APSK constellations for coherent optical channels with nonlinear phase noise," *IEEE Trans. Commun.*, vol. 61, no. 8, pp. 3362–3373, Aug. 2013.

[9] A. Ugolini, A. Piemontese, and T. Eriksson, "Spiral constellations for phase noise channels," *IEEE Trans. Commun.*, vol. 67, no. 11, pp. 7799–7810, Nov. 2019.

[10] S. Bicaïs and J.-B. Doré, "Phase noise model selection for sub-THz communications," in *Proc. IEEE Global Commun. Conf.*, Dec. 2019, pp. 1–6.

[11] L. Pometcu and R. D'Errico, "Characterization of Sub-THz and mmWave propagation channel for indoor scenarios," in *Proc. 12th Eur. Assoc. Antennas Propag.*, Apr. 2018, pp. 1–4, doi: 10.1049/cp.2018.0991.

[12] L. Pometcu and R. D'Errico, "Channel model characteristics in D-band for NLOS indoor scenarios," in *Proc. 13th Eur. Conf. Antennas Propag. (EuCAP)*, 2019, pp. 1–4.

[13] G. Gougeon, Y. Corre, and M. Z. Aslam, "Ray-based deterministic channel modelling for sub-THz band," in *Proc. IEEE Int. Symp. Personal, Indoor Mobile Radio Commun.*, Sep. 2019, pp. 1–6.

[14] M. Martalo, C. Tripodi, and R. Raheli, "On the information rate of phase noise-limited communications," in *Proc. Inf. Theory Appl. Workshop (ITA)*, Feb. 2013, pp. 1–7.

[15] A. G. Armada, "Understanding the effects of phase noise in orthogonal frequency division multiplexing (OFDM)," *IEEE Trans. Broadcasting*, vol. 47, no. 2, pp. 153–159, Jun. 2001.

[16] O. Tervo, T. Levanen, K. Pajukoski, J. Hulkkonen, P. Wainio, and M. Valkama, "5G new radio evolution towards Sub-THz communications," *2nd 6G Wireless Summit (6G SUMMIT)*, 2020, pp. 1–6, doi: 10.1109/6GSUMMIT49458.2020.9083807.

[17] A. Demir, "Computing timing jitter from phase noise spectra for oscillators and phase-locked loops with white and 1/f noise," *IEEE Trans. Circuits Syst. I: Regular Papers*, vol. 53, no. 9, pp. 1869–1884, Sep. 2006.

[18] M. R. Khanzadi, D. Kuylenstierna, A. Panahi, T. Eriksson, and H. Zirath, "Calculation of the performance of communication systems from measured oscillator phase noise," *IEEE Trans. Circuits Syst. I: Regular Papers*, vol. 61, no. 5, pp. 1553–1565, May 2014.

[19] S. Li, D. Fritsche, C. Carta, and F. Ellinger, "A 200-GHz sub-harmonic injection-locked oscillator with 0-dBm output power and 3.5 DC-to-RF-efficiency," in *Proc. IEEE Radio Freq. Integr. Circuits Symp.*, Jun. 2018, pp. 212–215.

[20] J. Proakis, *Digital Communications. in McGraw-Hill series in electrical and computer engineering : Communications and signal processing*, 5th Ed., New York, NY, USA; McGraw-Hill, 2007.

[21] R. Krishnan, M. R. Khanzadi, T. Eriksson, and T. Svensson, "Soft metrics and their performance analysis for optimal data detection in the presence of strong oscillator phase noise," vol. 61, no. 6, pp. 2385–2395, 2013.

[22] S. Bicaïs, J.-B. Doré, and J.-L. Gonzalez Jimenez, "On the optimum demodulation in the presence of Gaussian phase noise," in *Proc. Int. Conf. Telecommun.*, Jun. 2018, pp. 269–273, doi: 10.1109/ICT.2018.8464897.

[23] T. Moon and W. Stirling, *Mathematical Methods and Algorithms for Signal Processing*. Englewood Cliffs, NJ, USA; Prentice–Hall, 2000.

[24] F. Tosato and P. Bisaglia, "Simplified soft-output demapper for binary interleaved COFDM with application to HIPERLAN/2," in *Proc. IEEE Int. Conf. Commun.*, 2002, vol. 2, pp. 664–668.

[25] J. H. Lee and H. Chung, "Exact and approximate log-likelihood ratio of M-ary QAM with two-time dimensions," *ICT Express*, vol. 5, no. 3, pp. 173–177, 2019.

[26] *3rd Generation Partnership Project (3GPP)*, "Overall description stage 2," Technical Specification Group Access Network 38.300, 12 2017, 2.0.0.

[27] R. Hadani *et al.*, "Orthogonal time frequency space modulation," in *Proc. IEEE Wireless Commun. Netw. Conf.*, Mar. 2017, pp. 1–6.

[28] S. M. Kay, *Fundamentals of Statistical Signal Processing: Estimation Theory*. Englewood Cliffs, NJ, USA: Prentice-Hall, 1993.

[29] J. Horton Conway, N. J. A. Sloane, and E. Bannai, *Sphere Packings, Lattices and Groups*, Springer-Verlag, Berlin, Heidelberg, 1987, vol. 290.

[30] G. Forney, R. Gallager, G. Lang, F. Longstaff, and S. Qureshi, "Efficient modulation for band-limited channels," *IEEE J. Sel. Areas Commun.*, vol. 2, no. 5, pp. 632–647, Sep. 1984.

[31] M. Simon and J. Smith, "Hexagonal multiple phase-and-amplitude-shift-keyed signal sets," *IEEE Trans. Commun.*, vol. 21, no. 10, pp. 1108–1115, Oct. 1973.

[32] D. M. Arnold, H. Loeliger, P. O. Vontobel, A. Kavcic, and W. Zeng, "Simulation-based computation of information rates for channels with memory," *IEEE Trans. Inf. Theory*, vol. 52, no. 8, pp. 3498–3508, Aug. 2006.

[33] M. A. Tariq, H. Mehrpouyan, and T. Svensson, "Performance of circular QAM constellations with time varying phase noise," in *Proc. IEEE 23rd Int. Symp. Personal, Indoor Mobile Radio Commun.*, Sep. 2012, pp. 2365–2370.

[34] Z. Liu, Q. Xie, K. Peng, and Z. Yang, "APSK constellation with gray mapping," *IEEE Commun. Lett.*, vol. 15, no. 12, pp. 1271–1273, Dec. 2011.

[35] F. Schreckenbach, N. Gortz, J. Hagenauer, and G. Bauch, "Optimization of symbol mappings for bit-interleaved coded modulation with iterative decoding," *IEEE Commun. Lett.*, vol. 7, no. 12, pp. 593–595, Dec. 2003.

[36] S. Allpress, C. Luschi, and S. Felix, "Exact and approximated expressions of the log-likelihood ratio for 16-QAM signals," in *Proc. Conf. Record 38th Asilomar Conf. Signals, Syst. Comput.*, Nov 2004, vol. 1, pp. 794–798.

[37] A. Barre, E. Boutillon, N. Bias, and D. Diaz, "A polar-based demapper of 8PSK demodulation for DVB-S2 systems," in *Proc. SiPS* , Oct. 2013, pp. 13–17.

[38] T. Yoshida *et al.*, "Hardware-efficient precise and flexible soft-demapping for multi-dimensional complementary APSK signals," in *Proc. 42nd Eur. Conf. Opt. Commun.*, Sep. 2016, pp. 1–3.

[39] M. Zhang and S. Kim, "Efficient soft demapping for M-ary APSK," in *Proc. ICTC*, Sep. 2011, pp. 641–644.

[40] S. Bicaïs, J.-B. Doré, and J.-L. Gonzalez Jimenez, "Adaptive PSK modulation scheme in the presence of phase noise," in *Proc. Signal Process. Adv. Wireless Commun.*, Jun. 2018, pp. 1–5, doi: 10.1109/SPAWC.2018.8445933.

[41] J. Groe, "Polar transmitters for wireless communications," *IEEE Commun. Mag.*, vol. 45, no. 9, pp. 58–63, Sep. 2007.

[42] C. T. Chen, C. H. Hsiao, T. S. Horng, and K. C. Peng, "Wireless polar receiver using two injection-locked oscillator stages for green radios," in *Proc. IEEE MTT-S Int. Microw. Symp.*, Jun. 2011, pp. 1–4.

SIMON BICAÏS received the M.Sc. in telecommunications (2017), from the National Institute of Applied Sciences of Lyon (INSA Lyon), France. He is currently pursuing a Ph.D. in signal processing and communication systems at CEA-Leti, Grenoble, France. Signal processing, wireless communications and machine learning are his current research interests. He is involved in the BRAVE national project about Beyond 5G wireless communications in the sub-TeraHertz bands.

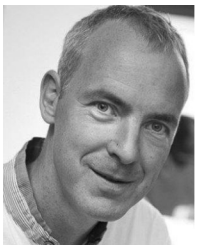

JEAN-BAPTISTE DORÉ received his MS degree in 2004 from the Institut National des Sciences Appliques (INSA) Rennes, France and his Ph.D. in 2007. He joined NXP semiconductors as a signal processing architect. Since 2009 he has been with CEA-Leti in Grenoble, France as a research engineer and program manager. His main research topics are signal processing (waveform optimization and channel coding), hardware architecture optimizations (FPGA, ASIC), PHY and MAC layers for wireless networks. Jean-Baptiste Doré has published 50+ papers in international conference proceedings and book chapters, received 2 best papers award (ICC2017, WPNC2018). He has also been involved in standardization group (IEEE1900.7) and is the main inventor of more than 30 patents.